

## Photoneutron Cross Section for ${}^4\text{He}$ up to 31 MeV\*

B. L. Berman, S. C. Fultz, and M. A. Kelly†

*Lawrence Radiation Laboratory, University of California, Livermore, California 94550*

(Received 13 May 1971)

The photoneutron cross section for  ${}^4\text{He}$  has been measured with monoenergetic photons from threshold to 31 MeV. The cross section reaches its maximum value of 1.0 mb from 24.3 to 27.3 MeV and appears to be split into two broad peaks. The integrated cross section is 7.9 MeV mb. The fore-aft asymmetry of the photoneutrons also was measured. This quantity, which is a measure of the interference between the  $E1$  amplitude and the underlying positive-parity contribution, changes from forward to backward peaking at about 27 MeV. The  $E2$ -to- $E1$  amplitude ratio deduced from these data is of the order of 0.04. A comparison of the cross-section results with the considerably larger values for the  ${}^4\text{He}(\gamma, p)$  reaction measured elsewhere shows appreciable ( $\approx 15\%$ ) isospin mixing throughout the energy region studied, with indications that this mixing might be increasing with energy above 28 MeV.

### I. INTRODUCTION

The study of the structure of the  ${}^4\text{He}$  nucleus is clearly of fundamental importance in nuclear physics. This nucleus is simple, consisting of only four nucleons, and is tightly bound. Its ground-state wave function must be predominantly a symmetric  $s$ -state configuration, so that one can hope to treat it fairly rigorously. It is self-conjugate and even-even, so that the electromagnetic selection rules dictate that only  $T=1$  states can be populated by  $E1$  or  $M1$  transitions, and only  $J^\pi = 1^-$  states can be populated by  $E1$  transitions. In the giant-resonance region, threshold and Coulomb-barrier effects are small, so that a straightforward treatment of photodisintegration cross-section and angular-distribution data should be possible. Even final-state interactions should be amenable to theoretical analysis, since the residual nuclei after photoemission of a nucleon, namely,  ${}^3\text{H}$  and  ${}^3\text{He}$ , are themselves simple nuclei.

Nevertheless, the present stage of understanding of this nucleus still is rudimentary. This stems largely from the fact that the experimental situation is a very difficult one: The cross sections are small, thus requiring high-pressure or cryogenic samples to be used, and the available data have been generally sketchy, confusing, and sometimes contradictory. This is particularly true for the  ${}^4\text{He}(\gamma, n)$  reaction: Only four measurements of this cross section in the energy range below about 40 MeV have been reported in the literature,<sup>1-4</sup> and all these have been made using continuous bremsstrahlung sources, with all the attendant difficulties and uncertainties. The present measurement of the  ${}^4\text{He}(\gamma, n)$  cross section from threshold to 31 MeV was made in an effort to remedy some of the shortcomings of the previous measurements. For the present experiment monoenergetic photons

were used; and the fore-aft asymmetry of the emitted photoneutrons also was measured, since this information bears on the multipolarity of the photoexcitation process.

### II. EXPERIMENTAL METHOD AND DATA REDUCTION

The monoenergetic photon beam used in the present experiment was obtained from the annihilation in flight of fast positrons from the Livermore linear electron accelerator. The techniques for the use of annihilation photons for photonuclear cross-section measurements have been described elsewhere.<sup>5</sup> Since most of the details of the experiment are the same as for similar measurements performed on  ${}^3\text{He}$ ,<sup>6</sup> only those details specific to the present measurement will be given here. Further experimental information will be given in a forthcoming publication.<sup>6</sup>

The liquid-helium sample was approximately 6 moles in mass, was 17 cm thick, and was contained in a Dewar vessel about 20 cm in diameter (see Fig. 1). The sample intercepted the entire collimated photon beam. The photon beam also passed through four thin (0.25-mm) aluminum windows, whose contribution to the total count rate was negligible.

The sample was located at the center of a  $4\pi$  neutron detector consisting of 48  $\text{BF}_3$  neutron detectors in a polyethylene moderator. This detector has been described by Kelly *et al.*<sup>7</sup> Its efficiency was measured by a variety of techniques, using calibrated neutron sources, spontaneous-fission coincidence measurements, and photoneutrons of known energy from  ${}^{12}\text{C}$  and  ${}^{89}\text{Y}$  (whose cross sections were measured previously at this laboratory<sup>5,8</sup>), and was found to vary smoothly from 24% for neutrons having an energy of 1 MeV to 17% for energies of 5 MeV and above for the case when the

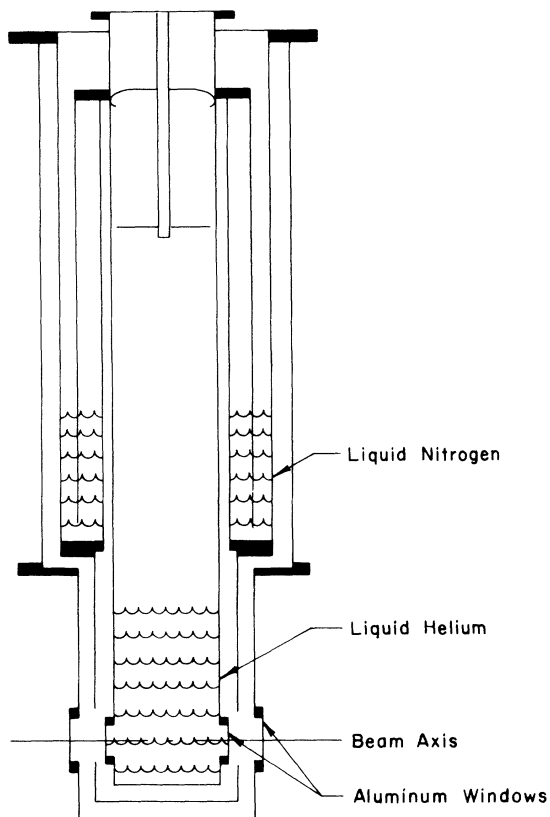


FIG. 1. The liquid-helium sample container. The Dewar vessel was surrounded by the  $4\pi$  polyethylene- and  $\text{BF}_3$ -tube neutron detector.

Dewar vessel did not contain helium (Fig. 2). The maximum systematic uncertainty in the detector efficiency is shown in Fig. 2 by the dashed lines, and varies from  $\pm 8\%$  at a neutron energy of 0.5 MeV, through  $\pm 2\%$  at 2 MeV to  $\pm 6\%$  at 7 MeV. In order to correct the detector efficiency for scattering effects when the helium sample was present, successive measurements under identical experimental conditions were made of the  $\text{C}(\gamma, n)$  cross section with and without helium in the Dewar vessel. This was done with a large (7.5-cm-diam by 13.8-cm-thick) graphite sample in the Dewar vessel which effectively displaced all the helium from the path of the photon beam. The results of these measurements are shown in Fig. 3, where the yield data both for positron and electron runs are shown. It is apparent that the presence of the helium column above the sample acts as a reflector for photoneutrons which otherwise would escape from the neutron detector and not be counted. This effect necessitated a correction to the detector efficiency (and hence to the cross-section data) which varied between 5.4 and 6.8%, depending upon the neutron energy. It should be noted that there is a one-to-one correspondence between neutron energy and photon energy for the reaction  ${}^4\text{He}(\gamma, n){}^3\text{He}$ , since there are no bound states of  ${}^3\text{He}$  below 5.5 MeV, and the  ${}^4\text{He}(\gamma, pn)$  cross section is known to be negligible below about 30 MeV<sup>9</sup>; hence the detector efficiency as a function of neutron energy translates directly into a function of photon energy.

The photon energy resolution was at most 400

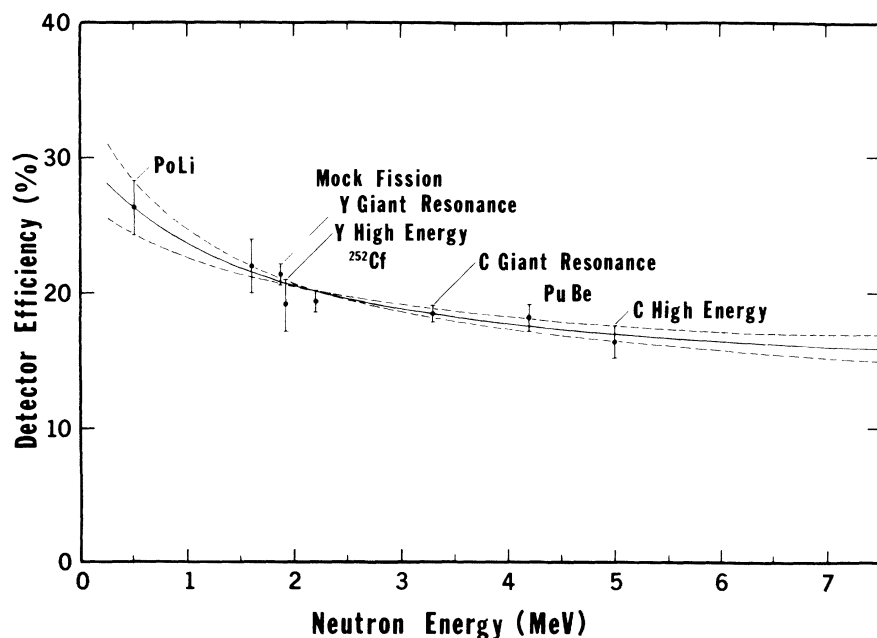


FIG. 2. The neutron-detector efficiency as a function of neutron energy (solid line). The dashed lines indicate the maximum systematic uncertainties.

keV, corresponding to the use of a 0.75-mm-thick beryllium annihilation target.<sup>10</sup> The energy scale and resolution were checked by a measurement of the 17.28-MeV peak<sup>11</sup> in the  ${}^{16}\text{O}(\gamma, n)$  cross section, using a water sample in the (room temperature) Dewar vessel (see Ref. 6). The absolute photon beam intensity was calibrated with the use of a 20 by 20-cm NaI(Tl) crystal.

The  ${}^4\text{He}(\gamma, n)$  data are shown in Fig. 4. These data have been corrected for backgrounds other than that caused by the direct photon beam, namely, neutron backgrounds originating from (a) cosmic rays and (b) the underground positron beam dump. These backgrounds were obtained from measurements performed before and after each data point taken with no annihilation target in the positron beam. A total of about  $5 \times 10^5$  events were recorded. The curve fitted to the electron data was used to subtract the neutron yield resulting from the positron bremsstrahlung from the total neutron yield for the positron runs in order to determine the yield resulting from the annihilation photons alone. Since the magnitude of the bremsstrahlung yield at the higher energies was somewhat uncer-

tain owing to the scatter of data points, a subsidiary measurement was performed with the high-intensity bremsstrahlung radiation source from the primary electron beam from the linac. These measurements were performed under otherwise identical conditions. The end-point energy was stepped from 29.6 to 42.2 MeV; the results up to 33 MeV also are shown (with arrows) in Fig. 4. These measurements also indicate that the cross section, while falling, is still appreciable at 40 MeV.

The net sample-blank (no helium) background is shown in Fig. 5. It is evident that the chief contributor to this background arises from the giant resonance of carbon, owing to the fringe region of the collimated photon beam striking the polyethylene moderator of the neutron detector. This is clear from the peak occurring at 22 to 23 MeV and the subsidiary shoulder at about 25.5 MeV.<sup>8</sup> The reason that the statistics for the sample-blank runs look poor is because the background is very small: The "arbitrary units" of the ordinates in Figs. 4 and 5 are the same. [Likewise, the data of Fig. 3, plotted with the same "arbitrary units,"

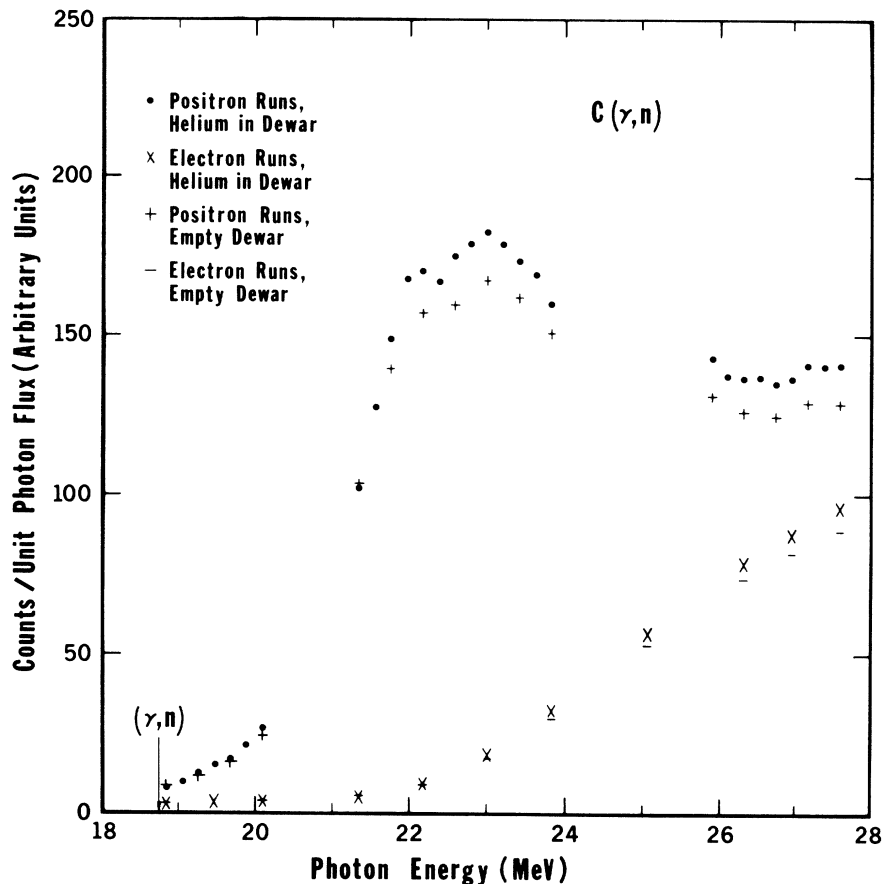


FIG. 3. Yield data for the  $\text{C}(\gamma, n)$  reaction, showing the effect on the detector efficiency of the presence of the  ${}^4\text{He}$  sample. The error bars are generally smaller than the size of the data points.

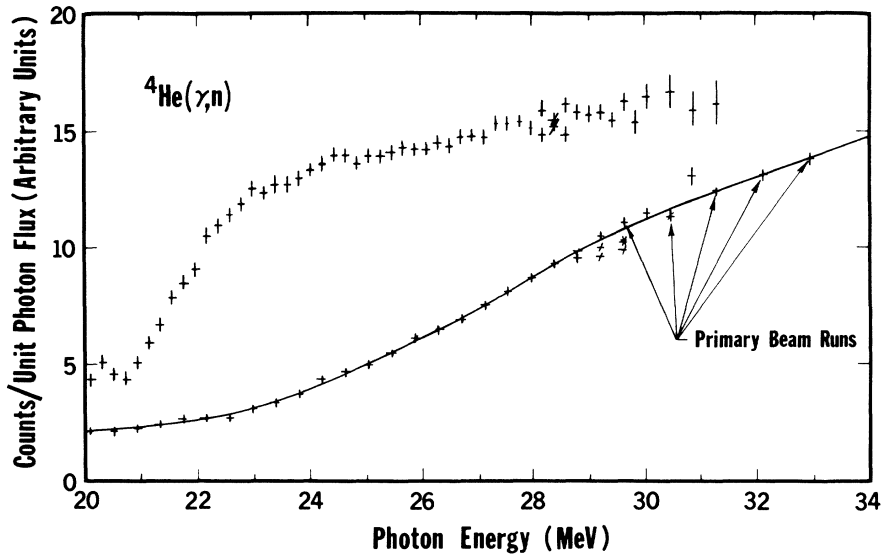


FIG. 4. The  ${}^4\text{He}(\gamma, n)$  data. The solid line fitted to the electron-run data was used as the measure of the neutron yield resulting from positron bremsstrahlung. The arrows indicate electron runs done with the primary linac beam. Certain data runs were repeated, as shown. The error bars represent statistical uncertainties only.

have excellent statistics (the error bars are generally smaller than the data points as shown), owing to the massive carbon sample used for those measurements.] The curve fitted to the sample-blank data in Fig. 5 was used to subtract the sample-out background from the net sample-in yield data obtained from Fig. 4.

The same procedure was followed in reducing the fore-aft photoneutron-asymmetry data. Since the neutron detector was divided into four sections, two forward of the laboratory angle  $90^\circ$  and two backward of it,<sup>7</sup> this asymmetry was measured simultaneously with the cross section. The

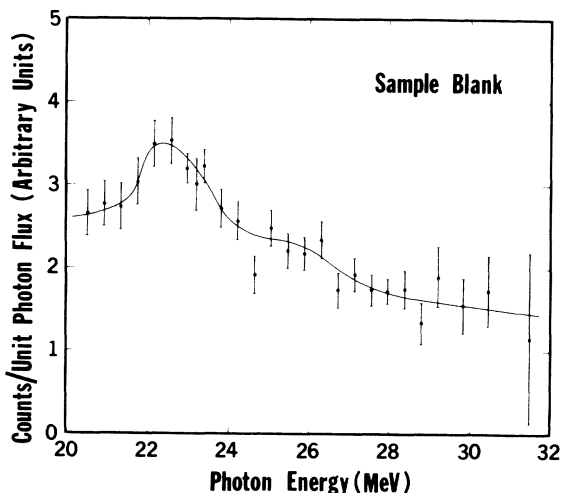


FIG. 5. The net sample-blank background. The solid line fitted to the data was subtracted from the net sample-in data to obtain the  ${}^4\text{He}(\gamma, n)$  yield.

neutron counting rates were measured for each detector quadrant separately. Then the data for the two forward quadrants, and for the two backward quadrants, were combined. Annihilation-target-out backgrounds were subtracted, curves were fitted to the electron data for both the sample-in and sample-blank cases, and net annihilation-photon neutron yields were obtained by subtraction from the positron data. The net sample-blank background then was subtracted from the net sample-in yield, and finally the ratio of the forward-to-backward counting rates was obtained. Although scattering of the photoneutrons in the sample or detector material during moderation could reduce the observed asymmetry so that these data represent a lower limit to the true asymmetry, such an effect is expected to be small.

### III. EXPERIMENTAL RESULTS AND DISCUSSION

#### A. Cross-Section Results

The  ${}^4\text{He}(\gamma, n)$  cross-section results are shown in Fig. 6. The error bars shown are statistical only. Systematic uncertainties are such that the absolute cross section might be in error by at most +15% or -10%. The cross section rises sharply from threshold, reaches its maximum value of 1.03 mb at about 24.3 MeV, is essentially flat up to about 27.3 MeV, where there is another slight indication of a peak, then decreases rapidly to about 0.55 mb at 31 MeV. The integrated cross section from threshold to 31.41 MeV is 7.94 MeV mb, about 13% of the electric dipole sum-rule value; its first moment  $\sigma_{-1}$  is 0.30 mb, and its second moment  $\sigma_{-2}$  is 0.012 mb MeV<sup>-1</sup>.

The  ${}^4\text{He}(\gamma, n)$  cross section measured in the present experiment up to about 27 MeV is somewhat smaller (but still within the experimental uncertainties) than the  $(\gamma, n)$  measurements of Ferguson *et al.*<sup>1</sup> and Ferrero *et al.*<sup>2</sup> and the  $(\gamma, {}^3\text{He})$  measurement of Busso *et al.*,<sup>4</sup> and somewhat larger than the  $(n, \gamma)$  measurement of Zurmühle, Stephens, and Staub,<sup>12</sup> but it disagrees strongly (about 40% lower) with the  $(\gamma, {}^3\text{He})$  measurement of Gorbunov.<sup>3</sup> Above this energy, the cross-section results of Refs. 2 and 4 rise to about 1.5 mb, whereas the present results indicate a decrease. The reasons for such discrepancies as exist between the present results and the various bremsstrahlung experiments are not clear. However, it should be noted that although there is a large discrepancy between the present results and those of Ref. 3, there is good agreement for the absolute cross section for the  ${}^3\text{He}(\gamma, n)$  reaction measured by both groups.<sup>6,13</sup>

Two broad  $J^\pi = 1^-, T = 1$  states, corresponding to singlet and triplet (or alternatively,  $p_{1/2}$  and  $p_{3/2}$ ) excitation are expected to dominate the photoabsorption cross section for  ${}^4\text{He}$  below 30 MeV.<sup>14</sup> It is clear from the shape of the cross section of Fig. 6 that this is likely to be the case. In an effort to demonstrate this splitting of the giant reso-

nance, a least-squares analysis was applied to the data, using Newton's method for the fitting procedure. The resonance shape was parametrized with noninterfering Breit-Wigner curves, assuming  $E1$  transitions and  $p$ -wave neutron decay and including threshold and centrifugal-barrier penetrability effects.<sup>15</sup> The results of this analysis are shown in Fig. 7. The dashed line is the best single-level fit achieved ( $\chi^2 = 1.22$ ), and the heavy solid line is the best fit ( $\chi^2 = 0.99$ ) using two levels. The light solid lines are the individual components of the two-level fit, and sum to the heavy line. The resonance energies obtained in this analysis are 30.9 MeV for the one-level fit and 26.3 and 28.0 MeV for the two-level fit.<sup>16</sup> (The fact that the cross-section curves peak at lower energies results from the energy dependence of the neutron widths.) These latter values agree well with the values predicted by several of the theoretical calculations,<sup>14</sup> but one should not place too much credence on the exact energies, since resonance energies a few hundred keV away yield fits that are not much worse. The best evidence, however, that two distinct states are populated is the fact that the fore-aft asymmetry of the photoneutrons (see below) changes sign between these two energies.

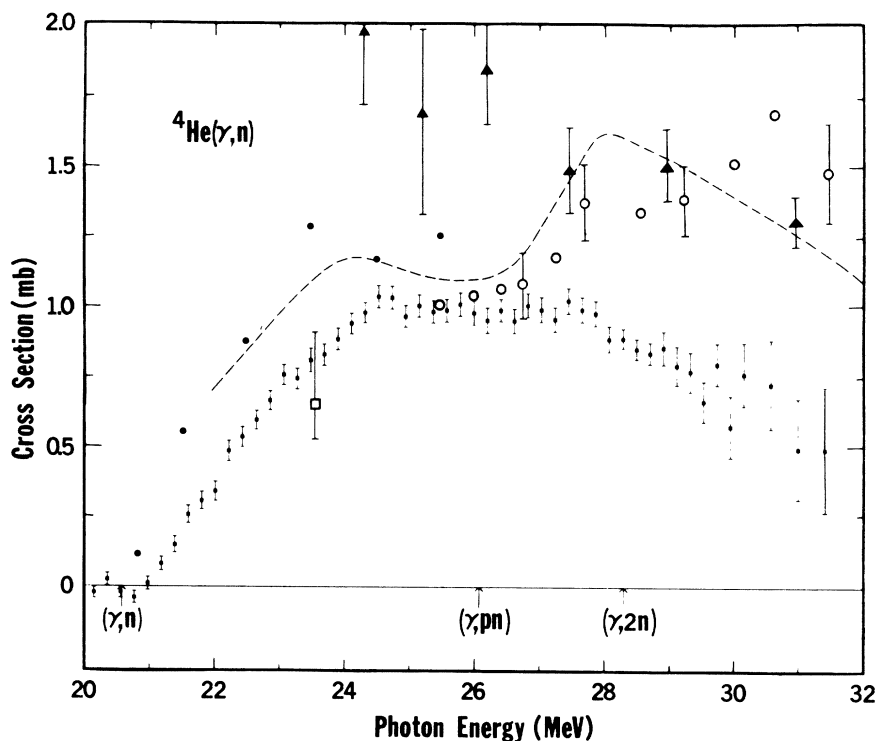


FIG. 6. The  ${}^4\text{He}(\gamma, n)$  cross section as a function of incident photon energy (closed squares). The arrows indicate threshold energies, as given in J. H. E. Mattauch, W. Thiele, and A. H. Wapstra, Nucl. Phys. 67, 32 (1965). The  ${}^4\text{He}(\gamma, n)$  data of Refs. 1 and 2 are shown as the closed circles and the dashed line, respectively; the  ${}^4\text{He}(\gamma, {}^3\text{He})$  data of Refs. 3 and 4 are shown as the triangles and the open circles, respectively; and the  ${}^3\text{He}(n, \gamma)$  datum of Ref. 12 is shown as the open square.

### B. Fore-Aft-Asymmetry Results

The results for the fore-aft asymmetry of the photoneutrons are shown in Fig. 8. The photoneutron asymmetry rises from zero near threshold to a strong forward peaking at about 23.5 MeV and then passes through zero again at about 27 MeV to an equally strong backward peaking at 30 MeV. No such asymmetry can be present without a mixture of both negative and positive parities. Therefore, between 23.5 and 30 MeV, there is a sign reversal in the interference between the dominant  $E1$  amplitude and the underlying positive-parity contribution. (The backward peaking of the photoneutrons above 27 MeV is confirmed by the angular-distribution data of Refs. 3 and 4.)

Since the photoprotons from the  ${}^4\text{He}(\gamma, p)$  reaction are peaked at forward angles throughout the giant-resonance region,<sup>3,17,18</sup> it appears that for the lower  $1^-$  state the photoneutrons and photoprotons in the final state interfere with the underlying positive-parity amplitude with the same phase, while for the upper  $1^-$  state they interfere with opposite phase.

The asymmetry coefficient  $\beta$  on the right-hand scale of Fig. 8 is computed under the assumption that the angular distribution is given by

$\sin^2\theta(1+\beta\cos\theta)$ . This would be the situation for the case that: (a) Only  $E1$  and  $E2$  photoabsorption were important; and (b) of the two possible channel spins  $S$  ( $S$  is defined as the vector sum of the final-state spins of the two outgoing particles), only  $S=0$  plays a role. The fragmentary angular-distribution data of Refs. 3 and 4 makes these simplifications plausible. Then a lower limit to the ratio of the  $E2$  to  $E1$  amplitudes is given by  $\frac{1}{10}\sqrt{3}\beta$ . For example, the value for this ratio at 23.5 MeV, where  $\beta \approx +0.2$ , is about 0.035; at 30 MeV, where  $\beta \approx -0.2$ , it is  $-0.035$ . This means that the  $E2$  contribution to the total  ${}^4\text{He}(\gamma, n)$  cross section is  $\approx 0.2\%$  ( $= \frac{1}{20}\beta^2$ ) of the  $E1$  intensity. If  $|\beta|=0.32$ , these quantities become  $\pm 0.055$  and  $0.5\%$ , respectively. For comparison, the value for the  $E2$ -to- $E1$  amplitude ratio deduced from the work of Busso *et al.*<sup>4,19</sup> is  $-0.023 \pm 0.012$  for the energy bin from 27 to 36 MeV, in satisfactory agreement with the present data. Thus, even the present crude fore-aft-asymmetry data serve to measure the very small  $E2$  amplitude involved. Of course, the fact that this amplitude is so small is not surprising, since an analysis based on the effective charges for  ${}^4\text{He}$  predicts the  $(\gamma, n)$   $E2$  amplitude to be only  $\frac{1}{5}$  of the  $(\gamma, p)$   $E2$  amplitude.<sup>20</sup> This is confirmed by the measurements of the corresponding  $E2$ -to-

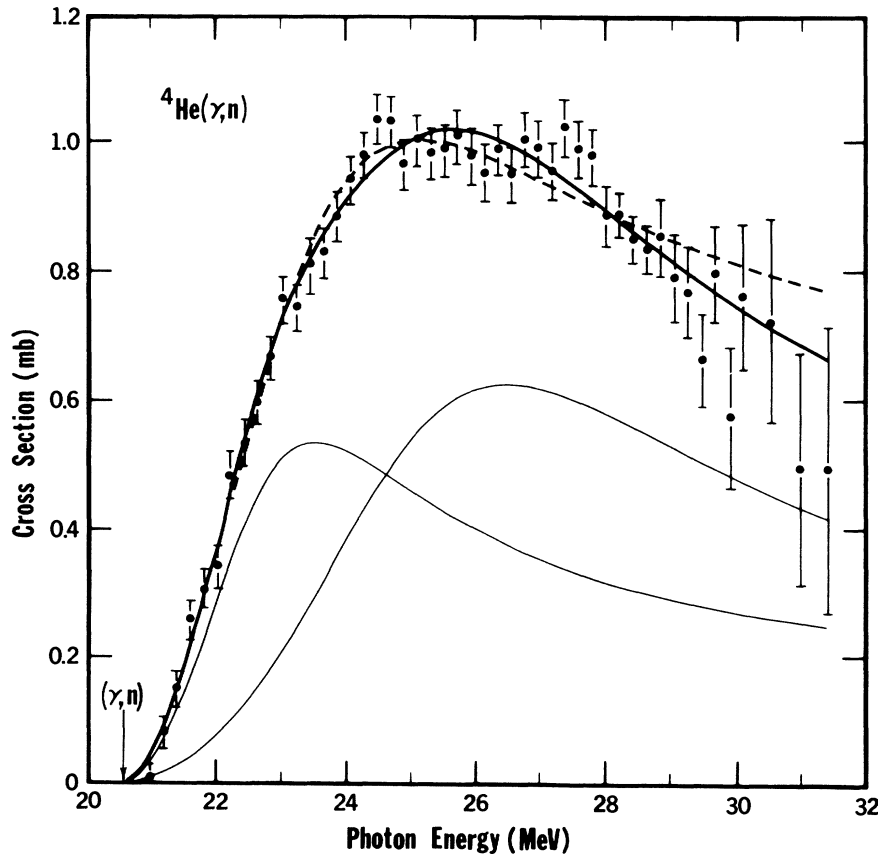


FIG. 7. The  ${}^4\text{He}(\gamma, n)$  cross section, fitted with one (dashed line) and with two (solid lines) noninterfering Breit-Wigner resonance curves. (See text.)

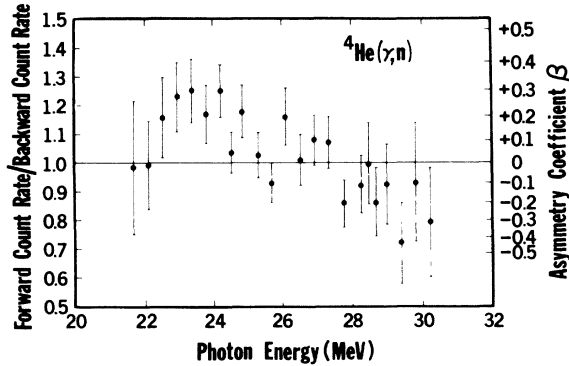


FIG. 8. The fore-aft asymmetry of the photoneutrons from  ${}^4\text{He}$  as a function of photon energy. The asymmetry coefficient  $\beta$  is computed on the assumption that the angular distribution is given by  $\sin^2\theta(1+\beta\cos\theta)$ .

$E1$  amplitude ratio for the  ${}^4\text{He}(\gamma, p)$  reaction, which is of the order of 0.15.<sup>17,18</sup> However, the effective-charge analysis predicts that the photoneutrons always will be peaked backwards, whereas this is the case only below 27 MeV.

### C. Isospin Mixing and Charge Symmetry

The question of isospin mixing in the giant dipole states of light nuclei is an intriguing one, and one that has begun to come under close scrutiny in recent years. In particular, Firk and collaborators<sup>21</sup> and Medicus *et al.*<sup>22</sup> have studied the self-conjugate nuclei  ${}^{12}\text{C}$ ,  ${}^{16}\text{O}$ ,  ${}^{28}\text{Si}$ ,  ${}^{32}\text{S}$ , and  ${}^{40}\text{Ca}$  by comparing their  $(\gamma, n)$  and  $(\gamma, p)$  cross sections. In none of these cases, however, can the nuclear-structure aspects of the problem be understood simply. Hence, the  ${}^4\text{He}$  nucleus, whose spectrum

of states up to 30 MeV or so is at least calculable in a relatively straightforward way,<sup>14</sup> takes on the aura of a special case: No other nucleus is so suitable for the study of isospin mixing.

Although numerous  ${}^4\text{He}(\gamma, p){}^3\text{H}$  measurements have been reported in the literature,<sup>3,4,23</sup> all were performed using a bremsstrahlung radiation source, several suffer from poor statistics, and in general the consistency between experiments is not good enough for a detailed energy-dependent analysis of the data. The experimental situation is far better for the  ${}^3\text{H}(p, \gamma){}^4\text{He}$  measurements,<sup>17,18,24,25</sup> however, in that all the measured cross-section curves are relatively smooth, have good statistics, and agree with each other. Nevertheless, the absolute peak  ${}^4\text{He}(\gamma, p)$  cross-section results of nearly all these measurements are in reasonable agreement with each other; the average value for this quantity is 1.8 mb, almost twice the present peak  ${}^4\text{He}(\gamma, n)$  cross section. Likewise, the integrated  $(\gamma, p)$  cross section up to 30 MeV is about twice the present  $(\gamma, n)$  value. This striking discrepancy was completely unexpected in a nucleus as simple as the  $\alpha$  particle, and can result from only two possibilities: (a) that there exists a large amount of Coulomb mixing, over a wide range of excitation energy, from strongly overlapping or nearly degenerate underlying  $T=0$  levels; or (b) that the  $n$ - $n$  interaction in the final state for the  ${}^4\text{He}(\gamma, n)$  process differs appreciably from the  $p$ - $p$  interaction in the final state for the  ${}^4\text{He}(\gamma, p)$  mirror process – a breaking of charge symmetry in nuclear interactions.

One can compute the isospin mixing ratio  $|a_0/a_1|$  in the giant resonance of  ${}^4\text{He}$ , whatever its origin

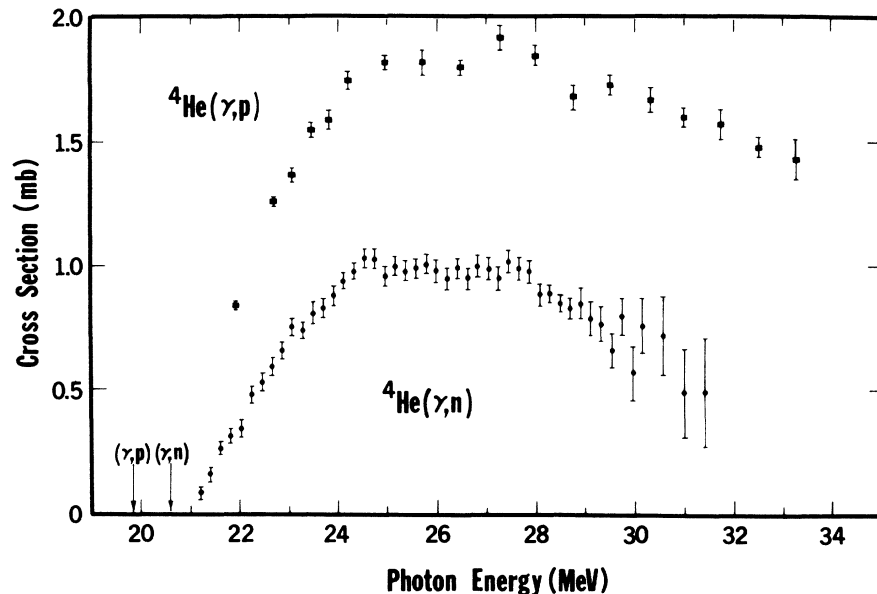


FIG. 9. The  ${}^4\text{He}(\gamma, p)$  cross section obtained from the  ${}^3\text{H}(p, \gamma)$  data of Meyerhof, Suffert, and Feldman (Ref. 18), together with the present  ${}^4\text{He}(\gamma, n)$  cross section.

(whether Coulomb or nuclear), from the relation<sup>26</sup>

$$\frac{\sigma(\gamma, n)}{\sigma(\gamma, p)} = \frac{P_n(E_n)}{P_p(E_p)} \left| \frac{a_1 - a_0}{a_1 + a_0} \right|^2,$$

where  $a_0$  and  $a_1$  are the amplitudes for the  $T=0$  and  $T=1$  components in the wave functions for the excited  ${}^4\text{He}$  giant-resonance states. The penetrabilities  $P_n(E_n)$  and  $P_p(E_p)$  are nearly equal to unity for energies more than a few MeV above the  $(\gamma, n)$  and  $(\gamma, p)$  thresholds at 19.8 and 20.6 MeV, respectively, so that above about 23 MeV, one can solve for  $|a_0/a_1|$  directly from the cross-section ratio  $R \equiv \sigma(\gamma, p)/\sigma(\gamma, n)$ :

$$|a_0/a_1| = (R^{1/2} - 1)/(R^{1/2} + 1).$$

Since a knowledge of the energy dependence of

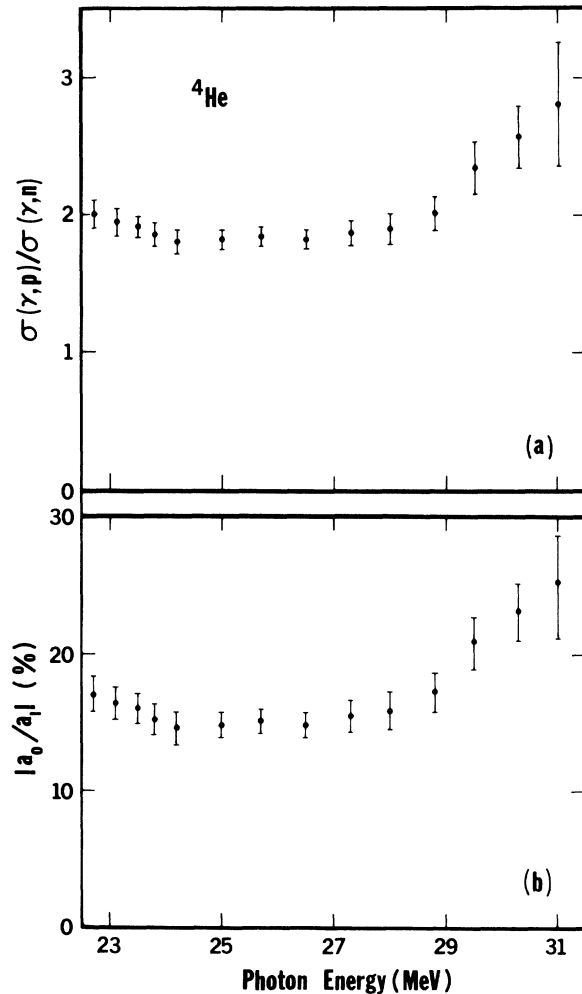


FIG. 10. (a) The ratio of the  ${}^4\text{He}(\gamma, p)$  to the  ${}^4\text{He}(\gamma, n)$  cross sections. The  $(\gamma, p)$  cross section used is a weighted average of the  $(p, \gamma)$  data of Refs. 17, 18, and 22. (b) The isospin-mixing ratio  $|a_0/a_1|$  obtained from the cross-section-ratio data of (a).

the mixing ratio might throw a good deal of light on the amount and shape of underlying  $T=0$  strength, the  $(p, \gamma)$  data were chosen to compare with the present data. The results of Meyerhof, Suffert, and Feldman<sup>18,27</sup> are shown in Fig. 9, together with the present  $(\gamma, n)$  cross section. One can see at a glance that the shapes are similar, even to the extent that the slight maximum at about 27.5 MeV appears in both cross sections. The data of Ref. 18 were then combined with those of Refs. 17 and 24, and a weighted average was obtained [except for the points above 29 MeV, for which Ref. 18 is the only  $(p, \gamma)$  experiment performed to date]. The resulting cross-section ratio  $R$  is plotted in Fig. 10(a), and the isospin mixing ratio  $|a_0/a_1|$  is plotted in Fig. 10(b). Both plots show almost no energy dependence across the main part of the giant-resonance region (24 to 28 MeV), but there is a definite upward trend above 29 MeV. (The slight rise at low energies might result from neglecting the penetrability ratio.) Even though both the statistical and systematic uncertainties in both experiments are largest at the highest energies, this 60% rise in  $|a_0/a_1|$  between 28 and 31 MeV appears to be beyond doubt (although it might be off by as much as a factor of 2 or so). Since, as mentioned above, the cross-section ratio  $R$  is expected to be equal to 5 for  $E2$  transitions, it is possible that a strong  $E2$  resonance lying near 31 MeV might be responsible for this rise, but the available evidence<sup>18,28</sup> indicates that this is not the case; and besides, the  $E2$  cross section required is enormous. Likewise, the magnitude of the  $\Delta T=0$ ,  $E1$  transition strength resulting from the non-zero momentum transfer to the nucleus  $q$  is small. The ratio of  $\Delta T=0$  to  $\Delta T=1$  amplitudes is  $\frac{1}{8}(qr)^3$  to  $qr$ , where  $r$  is the distance between the nucleon which absorbs the photon and the center of mass of the nucleus, approximately equal to the nuclear radius. For  $E_\gamma=30$  MeV and  $r=1.6$  F,  $\frac{1}{8}(qr)^2=0.01$ .

In any case, the value for  $|a_0/a_1|$  is very large at all energies, and where the data are best, equals 0.15. An effect of this magnitude is hard to explain by Coulomb mixing alone, especially since it appears to be nonresonant (unless the high-energy rise signifies the approach to a broad  $T=0$ ,  $J^\pi=1^-$  state). In fact, an estimate of the maximum Coulomb mixing with a broad underlying  $T=0$ ,  $J^\pi=1^-$  state can be obtained from the ratio of the Coulomb matrix element  $M_C$  to half the width  $\Gamma_0$  of the  $T=0$  state, under the assumption that the  $T=0$  state is completely degenerate with both  $T=1$  states; this implies that  $\Gamma_0 \geq 4$  MeV. One can set an upper limit on  $M_C$  of half the difference between the Coulomb energies of  $p$ -shell and  $s$ -shell protons in  ${}^4\text{He}$ , or about 400 keV; but since this value for  $M_C$  might very well be a factor of 2 or 3



too high,<sup>29</sup> and since the energy difference between the  $T=0$  state and at least one of the  $T=1$  states must make some contribution, then one expects  $|a_0/a_1|$  to be  $\leq 0.1$ . Moreover, this analysis fails utterly to explain the rise in  $|a_0/a_1|$  above 28 MeV, since the  $T=0$  state would have to lie near 27 MeV.

The alternative explanation – namely, a breaking of charge symmetry – presents equally formidable theoretical difficulties. It suffices to note that in absence of very appreciable and relatively constant Coulomb mixing across the entire giant-resonance region (or, probably less likely, an appreciable  $T=1$  admixture in the  ${}^4\text{He}$  ground state) there would have to be a charge-symmetry-breaking nuclear force leading to an intensity of the order of  $|a_0/a_1|^2 = 2.3\%$  of that resulting from the charge-symmetry-nonbreaking component. This should be compared with the value of  $\approx(0.25 \pm 0.80)\%$  given by Henley<sup>30</sup> from a summary of the low-energy scattering data. Further, it should be noted that the fact that such a small charge-symmetry-breaking force causes such a large difference in the mirror photoreactions illustrates the great sensitivity of this type of measurement. It should be noted, finally, that the main effect of  $E2$  photoabsorption, which can populate  $T=0$  states that can interfere with  $T=1$  states populated by  $E1$  absorption, is in

the angular distributions (because the interference term vanishes upon integration over all angles), and hence will not change the preceding argument concerning the breaking of charge symmetry.

#### IV. SUMMARY

The photoneutron cross section for  ${}^4\text{He}$  has been measured with monoenergetic photons from threshold to 31 MeV, together with the fore-aft asymmetry of the photoneutrons. The giant resonance appears to be split into two broad  $J^\pi = 1^-$  states at about 26 and 28 MeV, and they interfere, with opposite phase, with a small ( $\approx 4\%$ ) underlying  $E2$  amplitude. Comparison with  ${}^4\text{He}(\gamma, p)$  data indicates a large ( $\approx 15\%$ ) isospin mixing throughout the giant-resonance region, and the mixing ratio appears to rise appreciably above 28 MeV.

#### ACKNOWLEDGMENTS

The authors thank C. N. Orton for help in taking the data, G. L. Godfrey for help in the analysis, E. Dante and staff for the accelerator operation, and Dr. B. F. Gibson, Dr. A. Goldberg, Dr. A. K. Kerman, Dr. T. W. Phillips, and Dr. M. S. Weiss for valuable discussions.

\*Work performed under the auspices of the U. S. Atomic Energy Commission. A preliminary account of this work appeared as *Phys. Rev. Letters* **25**, 938 (1970).

†Present address: Hewlett-Packard Corporation, Palo Alto, California 94304.

<sup>1</sup>G. A. Ferguson, J. Halpern, R. Nathans, and P. F. Yergin, *Phys. Rev.* **95**, 776 (1954).

<sup>2</sup>F. Ferrero, C. Manfredotti, L. Pasqualini, G. Piragino, and P. G. Rama, *Nuovo Cimento* **45B**, 273 (1966).

<sup>3</sup>A. N. Gorbunov, *Phys. Letters* **27B**, 436 (1968).

<sup>4</sup>L. Busso, S. Costa, L. Ferrero, R. Garfagnini, L. Pasqualini, G. Piragino, S. Ronchi della Rocca, and A. Zanini, *Lettere Nuovo Cimento* **3**, 423 (1970); L. Busso, R. Garfagnini, G. Piragino, S. Ronchi della Rocca, and A. Zanini, private communication.

<sup>5</sup>B. L. Berman, J. T. Caldwell, R. R. Harvey, M. A. Kelly, R. L. Bramblett, and S. C. Fultz, *Phys. Rev.* **162**, 1098 (1967), and references therein.

<sup>6</sup>B. L. Berman, S. C. Fultz, and P. F. Yergin, *Phys. Rev. Letters* **24**, 1494 (1970); to be published.

<sup>7</sup>M. A. Kelly, B. L. Berman, R. L. Bramblett, and S. C. Fultz, *Phys. Rev.* **179**, 1194 (1969).

<sup>8</sup>S. C. Fultz, J. T. Caldwell, B. L. Berman, R. L. Bramblett, and R. R. Harvey, *Phys. Rev.* **143**, 790 (1966).

<sup>9</sup>A. N. Gorbunov and V. M. Spiridonov, *Zh. Eksperim. i Teor. Fiz.* **34**, 866 (1958) [transl.: *Soviet Phys.-JETP* **34**, 600 (1958)]; Yu. M. Arkatov, A. V. Bazaeva, P. I. Vatsset, V. I. Voloshchuk, A. P. Klyucharev, and A. F. Khodyachikh, *Yadern. Fiz.* **10**, 1123 (1969) [transl.: *Soviet J. Nucl. Phys.* **10**, 639 (1970)].

<sup>10</sup>R. L. Bramblett, J. T. Caldwell, B. L. Berman, R. R. Harvey, and S. C. Fultz, *Phys. Rev.* **148**, 1198 (1966).

<sup>11</sup>F. W. K. Firk, private communication.

<sup>12</sup>R. W. Zurmühle, W. E. Stephens, and H. H. Staub, *Phys. Rev.* **132**, 751 (1963). An error was made in the detailed-balance calculation in *Phys. Rev. Letters* **25**, 938 (1970): The  $(n, \gamma)$  result yields a  $(\gamma, n)$  cross section of  $0.64^{+0.25}_{-0.13}$  mb at 23.6 MeV, compared with the present result of 0.82 mb at that energy.

<sup>13</sup>V. N. Fetsiov, A. N. Gorbunov, and A. T. Varfolomeev, *Nucl. Phys.* **71**, 305 (1965).

<sup>14</sup>W. E. Meyerhof and T. A. Tombrello, *Nucl. Phys.* **A109**, 1 (1968); I. Sh. Vashakidze and V. I. Mamasakhlishvili, *Yadern. Fiz.* **6**, 732 (1967) [transl.: *Soviet J. Nucl. Phys.* **6**, 532 (1968)]; G. Sh. Gogsadze and T. I. Kopaleishvili, *Yadern. Fiz.* **8**, 875 (1968) [transl.: *Soviet J. Nucl. Phys.* **8**, 509 (1969)]; P. P. Szydlik, *Phys. Rev. C* **1**, 146 (1970).

<sup>15</sup>J. M. Blatt and V. F. Weisskopf, *Theoretical Nuclear Physics* (John Wiley & Sons, New York, 1952), Chap. VIII. A square-well potential was used with well parameters of 75.4 MeV and 1.74 F, as used by J. Hüfner and C. M. Shakin, *Phys. Rev.* **175**, 1350 (1968).

<sup>16</sup>These values supersede the preliminary values given in *Phys. Rev. Letters* **25**, 938 (1970).

<sup>17</sup>D. S. Gemmel and G. A. Jones, *Nucl. Phys.* **33**, 102 (1962).

<sup>18</sup>W. E. Meyerhof, M. Suffert, and W. Feldman, *Nucl. Phys.* **A148**, 211 (1970).

<sup>19</sup>Deduced from the  $a_3/a_2$  ratio of Ref. 4.

- <sup>20</sup>E. Hayward, in *Nuclear Structure and Electromagnetic Interactions*, edited by N. MacDonald (Plenum Press, Inc., New York, 1965), p. 145.
- <sup>21</sup>C.-P. Wu, F. W. K. Firk, and T. W. Phillips, *Phys. Rev. Letters* **20**, 1182 (1968); C.-P. Wu, J. E. E. Baglin, F. W. K. Firk, and T. W. Phillips, *Phys. Letters* **29B**, 359 (1969); C.-P. Wu, F. W. K. Firk, and T. W. Phillips, *Nucl. Phys.* **A147**, 19 (1970).
- <sup>22</sup>H. A. Medicus, E. M. Bowey, D. B. Gayther, B. H. Patrick, and E. J. Winhold, *Nucl. Phys.* **A156**, 257 (1970).
- <sup>23</sup>E. G. Fuller, *Phys. Rev.* **96**, 1306 (1954); H. G. Clerc, R. J. Stewart, and R. C. Morrison, *Phys. Letters* **18**, 316 (1965); V. P. Denisov and L. A. Kul'chitskii, *Yadern. Fiz.* **6**, 437 (1967) [transl.: *Soviet J. Nucl. Phys.* **6**, 319 (1968)]; R. Mundhenke, R. Kosiek, and G. Kraft, *Z. Physik* **216**, 232 (1968); J. Sanada, M. Yamanouchi, N. Sakai, and S. Seki, *J. Phys. Soc. Japan* **28**, 537 (1970); Yu. M. Arkatov, P. I. Vatset, V. I. Voloshchuk, V. V. Kirichenko, I. M. Prokhorets, and A. F. Khodyachikh, *Zh. Eksperim. i Teor. Fiz. - Pis'ma Redakt.* **9**, 574 (1969) [transl.: *JETP Letters* **9**, 350 (1969)]; G. D. Wait, S. K. Kundu, Y. M. Shin, and W. F. Stubbins, *Phys. Letters* **33B**, 163 (1970).
- <sup>24</sup>J. E. Perry, Jr., and S. J. Bame, Jr., *Phys. Rev.* **99**, 1368 (1955).
- <sup>25</sup>C. C. Gardner and J. D. Anderson, *Phys. Rev.* **125**, 626 (1962).
- <sup>26</sup>F. C. Barker and A. K. Mann, *Phil. Mag.* **2**, 5 (1957).
- <sup>27</sup>The  ${}^3\text{H}(p, \gamma)$  90° differential-cross-section data of Ref. 18 were normalized to the absolute data of Ref. 22, and the conversion to the total cross section was made with the aid of the 0°/90° yield ratios of Ref. 18. However, there is a slight mistake in the conversion formula in Ref. 18 [Eq. (4)]; correcting the error would raise the  $\sigma(\gamma, p)$  values by about 3%, nearly uniformly over the giant-resonance region. This correction is *not* made here.
- <sup>28</sup>W. E. Meyerhof, W. Feldman, S. Gilbert, and W. O'Connell, *Nucl. Phys.* **A131**, 489 (1969).
- <sup>29</sup>B. F. Gibson, private communication.
- <sup>30</sup>E. M. Henley, in *Isospin in Nuclear Physics*, edited by D. H. Wilkinson (North-Holland Publishing Company, Amsterdam, The Netherlands, 1969), p. 43.

## Mass Formula Consistent with Nuclear-Matter Calculations vs Conventional Mass-Law Extrapolations\*

K. A. Brueckner, J. H. Chirico, and H. W. Meldner

*Institute for Pure and Applied Physical Sciences, University of California at San Diego, La Jolla, California 92037*  
(Received 5 May 1971)

The energy-density functional proposed by Brueckner *et al.* is used to calculate the average nuclear-binding-energy surface on the  $N$ - $Z$  plane at  $\beta$  stability  $\pm$  about 40 units. The equi-binding contours are compared with those predicted by recent liquid-droplet models. Normally, some disagreement begins about 15 units away from the region of known nuclei. The deviations towards *lower* binding are significant for neutron-rich transuranium (superheavy) nuclei. This would seem to indicate a physically important uncertainty in conventional mass-law extrapolations. The semiempirical dependence on neutron excess cannot be established very well, because of the narrowness of the region of known isotopes. The energy-density functional, on the other hand, incorporates the present knowledge about nuclear matter - including recent neutron-matter results. Our disagreement with other extrapolations, therefore, questions the validity of stability and formation (e.g.,  $r$ -process) calculations based on conventional mass formulas.

### I. INTRODUCTION

The conventional mass formula describes the nuclear binding energy with a *function*  $E(A, Z)$ , whereas the energy-density formalism<sup>1-4</sup> gives it as a *functional*  $E[\rho, \rho_p]$ , with  $\rho$  and  $\rho_p$  normalized to  $A$  and  $Z$ , respectively. One major advantage of the explicit functional dependence on density distributions, is, of course, the possibility to calculate the shape dependence of nuclear binding (cf. Ref. 4). Also of practical importance are cases where the total and proton density profiles are very different from those of known nuclei.

This paper is concerned with such situations, i.e., extrapolations from the region of existing isotopes to superheavy nuclei and areas of astrophysical interest. The energy-density functional clearly makes a more complete use of nuclear-matter results than semiempirical mass formulas and is thus expected to allow more reliable extrapolations.

Naturally, the degree to which it is better than conventional mass formulas depends on the quality of the input. It is crucial to understand *quantitatively* the nuclear-matter limit where  $E$  is no longer a functional but just a function of the constant (translationally invariant) density compo-